

Received: 2020.09.24

Accepted: 2020.10.11

Available online: 2020.10.29

Published: 2020.12.18

Functional Analysis of Estrogen Receptor 1 in Diabetic Wound Healing: A Knockdown Cell-Based and Bioinformatic Study

Authors' Contribution:

Study Design A
Data Collection B
Statistical Analysis C
Data Interpretation D
Manuscript Preparation E
Literature Search F
Funds Collection G

ABC **Sha Qi**
BC **Qiong Han**
D **Danmou Xing**
CE **Long Qian**
E **Xiang Yu**
F **Dong Ren**
E **Huan Wang**
ABFG **Quan Chen**

Department of Hand Surgery, Wuhan Fourth Hospital; Puai Hospital, Tongji Medical College, Huazhong University of Science and Technology, Wuhan, Hubei, P.R. China

Corresponding Author: Quan Chen, e-mail: 382326563@qq.com

Source of support: Departmental sources

Background: Diabetic wound (DW) treatment is a serious challenge for clinicians, and the underlying mechanisms of DWs remain elusive. We sought to identify the critical genes in the development of DWs and provide potential targets for DW therapies.

Material/Methods: Datasets of GSE38396 from the Gene Expression Omnibus (GEO) database were reviewed. Pathway analysis was performed using the Kyoto Encyclopedia of Genes and Genomes (KEGG), Gene Ontology term analyses were carried out, and Cytoscape software (Cytoscape 3.7.2) was used to construct the protein interaction network. Serum samples from patients with diabetes and control participants were collected, and the expression of estrogen receptor 1 (ESR1) was measured by quantitative reverse-transcription polymerase chain reaction. In addition, the function of ESR1 in human skin fibroblasts was investigated *in vitro*.

Results: Eight samples were analyzed using the Morpheus online tool, which identified 637 upregulated and 448 down-regulated differentially expressed genes. The top 5 KEGG pathways of upregulated differentially expressed genes were associated with sphingolipid metabolism, estrogen signaling, ECM-receptor interaction, MAPK signaling, and PI3K-Akt signaling. The hub genes for DWs were *JUN*, *ESR1*, *CD44*, *SMARCA4*, *MMP2*, *BMP4*, *GSK3B*, *WDR5*, *PTK2*, and *PTGS2*. *JUN*, *MMP2*, and *ESR1* were the upregulated hub genes, and *ESR1* was found to be consistently enriched in DW patients. Inhibition of *ESR1* had a stimulative role in human skin fibroblasts.

Conclusions: *ESR1* was identified as a crucial gene in the development of DWs, which suggests potential therapeutic targets for DW healing.

MeSH Keywords: **Diabetic Angiopathies • Fibroblasts • Genes, vif**

Full-text PDF: <https://www.medscimonit.com/abstract/index/idArt/928788>

 2251

 6

 8

 26



Background

It is widely accepted that a diagnosis of diabetes requires a substantial change in dietary habits and can produce overwhelming mental and social stress [1]. In addition, neurovascular lesions, secondary infection, hypoxia, and other harmful factors can cause diabetic wounds (DWs) that are challenging for clinicians to treat. Further, because these lesions are usually incurable, they cause economic and psychological burdens for patients [2]. A large number of studies have focused on the potential mechanisms underlying DW development [3]. For example, a recent study reported that circulating microRNA-20b-5p derived from the serum of patients with diabetes is associated with the deterioration of DWs, thereby providing a new therapeutic target for their treatment [4]. Similarly, a study regarding the therapeutic strategies for diabetic foot ulcers indicated that exosomal microRNA-15a-3p plays a crucial role in regulation of the healing progress through the NOX5/ROS signaling pathway [5]. Although many studies regarding DWs have been carried out, a clear mechanism for their development remains elusive.

Regulatory factors *in vivo* affect the angiogenesis and the ability of a wound to resist infection. The regeneration of tissue around a wound plays a crucial role in the healing process of DW, and various regulatory genes can directly or indirectly modulate this process. For instance, ubiquitin-conjugating enzyme E2 (UBE2O) derived from salivary exosomes was reported to accelerate wound repair via targeting decapentaplegic homolog 6 (SMAD6) [6]. It was similarly reported that palmitate-TLR4 signaling plays a key regulatory role in DW healing via targeting the histone demethylase (JMJD3) [7]. Therefore, DWs are thought to be related to multiple regulatory genes and caused by gene-environment interactions.

A DNA microarray (also commonly known as DNA chip or biochip) is a collection of microscopic DNA spots attached to a solid surface. Such microarrays have been used to investigate the underlying pathogenic processes in a variety of diseases, and they have become crucial in functional genomic studies [8–10]. This technique has been widely applied to identify significant regulatory genes in diabetic diseases [11]. The differentially expressed genes (DEGs) are assumed to be related to changes in the levels of proteins that have significant functionality in this context and thus to have important regulatory effects in the progression of diabetes-related diseases. Therefore, we sought to identify critical DEGs in the development of DWs by using a comprehensive method based on bioinformatics.

Material and Methods

Gene chip data acquisition

The Gene Expression Omnibus (GEO; <https://www.ncbi.nlm.nih.gov/gds>) repository is a database of high-throughput gene expression data and hybridization arrays, chips, and microarrays. We searched this database for the RNA microarray data comparing people with type 2 diabetes with a normal population. We then downloaded the files.

Identification of DEGs

Morpheus (<https://software.broadinstitute.org/morpheus>) is an online software for data visualization and analysis. We uploaded reorganized GEO data to this online tool. A heat map produced by Morpheus sorted the DEGs with signal to noise >1 or signal to noise <-1.

Enrichment analyses of Gene Ontology and Kyoto Encyclopedia of Genes and Genomes pathways

The online tool Database for Annotation, Visualization, and Integrated Discovery version (DAVID) Bioinformatics Resources 6.8 was used to the biological function of the genes [12,13]. Gene Ontology (GO) enrichment and Kyoto Encyclopedia of Genes and Genomes (KEGG) pathway analyses were performed with DAVID.

Protein–protein interaction network construction

Upregulated and downregulated genes were imported into the software STRING (Search Tool for the Retrieval of Interacting Genes, <https://string-db.org/>), which identified the genes with a combined score of >0.5. (This score is based on the likelihood of interaction, and >0.5 is the default value.) Subsequently, the protein–protein interaction (PPI) network was constructed using Cytoscape software (version 3.7.2) [14]. Next, an analysis of the function enrichment was performed using DAVID, and the DEGs were ranked by degree centrality using the plugin software Centiscape 2.2 in Cytoscape. Degree represents the degree to which one node is associated with all other nodes in the network. Closeness represents how close a node is to other nodes in the network. Betweenness is the number of times that a node acts as the shortest bridge between 2 other nodes.

Ethics approval

The present study was approved by the Committees of Ethics in Wuhan Fourth Hospital (Wuhan, Hubei, China; 2019-021-17).

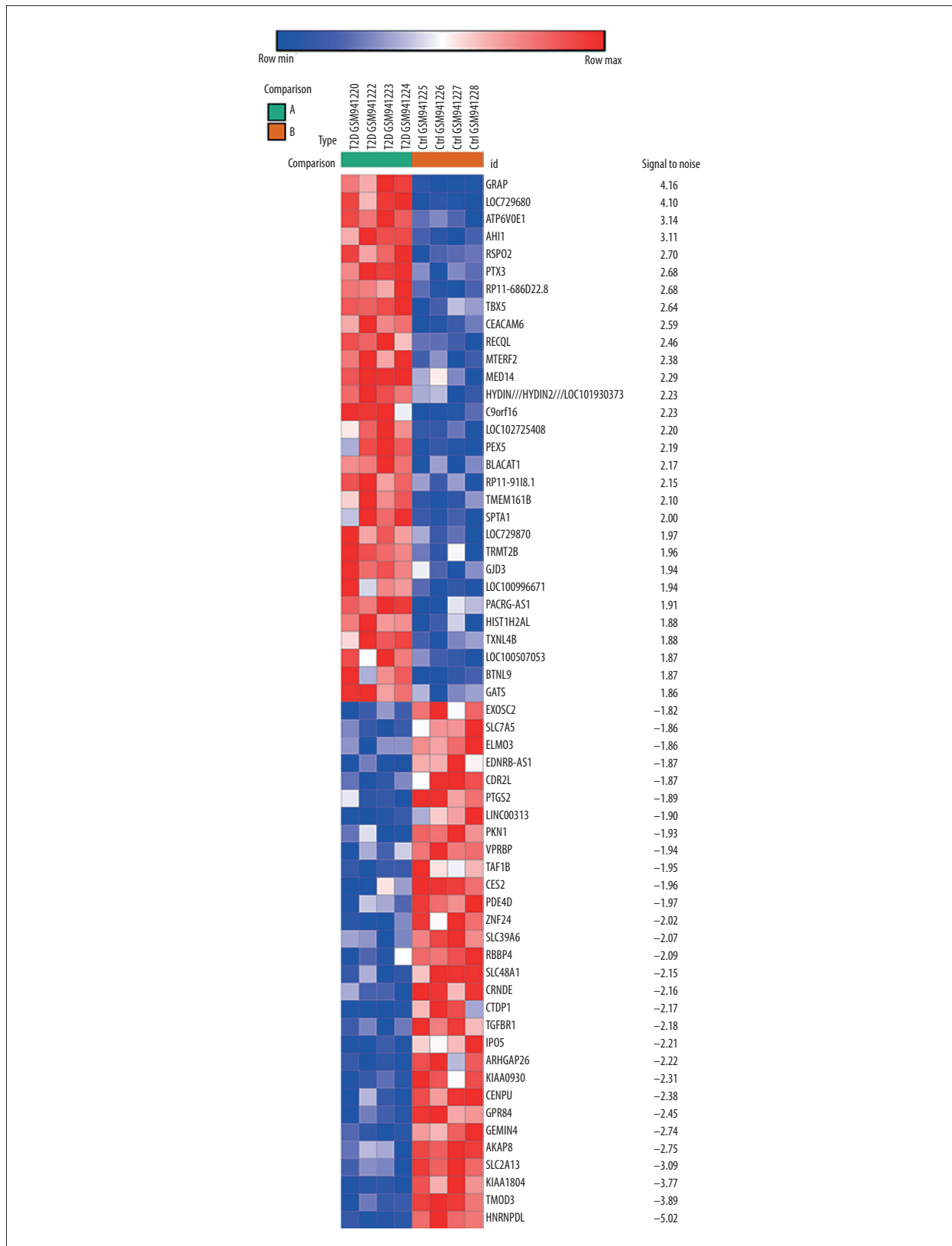


Figure 1. The top 60 differentially expressed genes (DEGs) of GSE38396 (30 upregulated and 30 downregulated) are presented in the heat map.

Table 1. The upregulated and downregulated differentially expressed genes (DEGs) in biological process.

Term	Function	Count	P-value
Upregulated			
GO: 0043547	Positive regulation of GTPase activity	32	3.0E-4
GO: 0072358	Cardiovascular system development	42	4.1E-4
GO: 0072359	Circulatory system development	42	4.1E-4
GO: 0051345	Positive regulation of hydrolase activity	40	8.4E-4
GO: 0007507	Heart development	26	1.1E-3
Downregulated			
GO: 0008283	Cell proliferation	70	1.4E-6
GO: 0048608	Reproductive structure development	26	2.6E-6
GO: 0061458	Reproductive system development	26	3.2E-6
GO: 0008285	Negative regulation of cell proliferation	32	1.8E-5
GO: 0010605	Negative regulation of macromolecule metabolic process	77	3.7E-5

Table 2. The upregulated and downregulated differentially expressed genes (DEGs) in cellular component.

Term	Function	Count	P-value
Upregulated			
GO: 0031904	Endosome lumen	6	4.8E-4
GO: 0044447	Axoneme part	5	4.2E-3
GO: 0005788	Endoplasmic reticulum lumen	13	6.6E-3
GO: 0005775	Vacuolar lumen	9	1.1E-2
GO: 0031906	Late endosome lumen	3	1.3E-2
Downregulated			
GO: 0005654	Nucleoplasm	105	2.4E-7
GO: 0044451	Nucleoplasm part	31	8.8E-4
GO: 0005912	Adherens junction	29	1.4E-3
GO: 0070161	Anchoring junction	29	2.0E-3
GO: 0001725	Stress fiber	6	6.4E-3

Sample collection from patients and healthy controls

From April 2019 to March 2020, peripheral blood samples from patients with DWs and healthy controls in our hospital (30 non-diabetic patients with foot trauma, and 30 diabetic patients with foot ulcers) were obtained for the subsequent validation of mRNA levels of the upregulated hub genes.

Cell culture and transfection

Human skin fibroblasts (HSFs; FuHeng Biology, Shanghai, China) were cultured in high-glucose Dulbecco's modified Eagle's medium (Gibco BRL, Grand Island, NY, USA) with 10% fetal bovine serum. For transfection, Lipofectamine 3000 (ThermoFisher Scientific) was used following the manufacturer's instructions.

Briefly, cells were cultured at 37°C with 5% CO₂ and 95% humidity. For the transfection of mRNA and siRNA oligos steps, constructs from RIBOBIO (Guangzhou) were utilized, and cells were transfected with ESR1 siRNA (RIBOBIO, Guangzhou) at 50 nM.

Quantitative reverse-transcription polymerase chain reaction analyses

The total RNA was obtained from the serum samples. cDNA was then obtained through reverse and transcribe of the purified RNA. GAPDH served as an internal control. Relative miRNA expression levels were normalized to those of the internal control and were calculated according to the 2^{-ΔΔC_t} approach. The primer sequences were as follows: ESR1, forward, GACAGGGAGCTGGTTCACAT,

Table 3. The upregulated and downregulated differentially expressed genes (DEGs) in molecular function.

Term	Function	Count	P-value
Upregulated			
GO: 0005085	Guanyl-nucleotide exchange factor activity	17	3.1E-3
GO: 0098772	Molecular function regulator	50	4.2E-3
GO: 0005088	Ras guanyl-nucleotide exchange factor activity	13	8.8E-3
GO: 0052745	Inositol phosphate phosphatase activity	4	9.9E-3
GO: 0030170	Pyridoxal phosphate binding	6	1.2E-2
Downregulated			
GO: 0044822	Poly(A) RNA binding	50	7.8E-6
GO: 0000166	Nucleotide binding	80	3.4E-5
GO: 1901265	Nucleoside phosphate binding	80	3.4E-5
GO: 0036094	Small molecule binding	82	1.4E-4
GO: 0097367	Carbohydrate derivative binding	73	2.0E-4

Table 4. The Kyoto Encyclopedia of Genes and Genomes analysis of upregulated and downregulated differentially expressed genes (DEGs).

Term	Function	Count	P-value
Upregulated			
hsa00600	Sphingolipid metabolism pathway	6	5.3E-3
hsa04915	Estrogen signaling pathway	8	1.0E-2
hsa04512	ECM-receptor interaction pathway	7	1.9E-2
hsa04010	MAPK signaling pathway	13	2.0E-2
hsa04151	PI3K-Akt signaling pathway	16	2.0E-2
Downregulated			
hsa04390	Hippo signaling pathway	11	6.1E-4
hsa04350	TGF-beta signaling pathway	6	2.2E-2
hsa03015	mRNA surveillance pathway	6	3.0E-2
hsa04152	AMPK signaling pathway	7	3.1E-2
hsa04360	Axon guidance pathway	7	3.5E-2

reverse, AGGATCTCTAGCCAGGCACA;
cyclin D1, forward, TTGCCCTCTGTGCCACAGAT,
reverse, TCAGGTTTCAGGCTTGCACT;
cyclin D3, forward, CTGCCATGAACTACCTGGA,
reverse, CCAGCAAATCATGTGCAATC;
Bcl-2, forward, GATAACGGAGGCTGGGATGC,
reverse, TCACTTGTGGCCAGATAGG;
Bax, forward, CCCTTTGCTTCAGGGTTTC,
reverse, GAGACACTCGCTCAGCTTCTTG;
GAPDH, forward, TCGACAGTCAGCCGCATCTTCTT,
reverse, GCCCAATACGACCAAATCCGTTGA.

Cell Counting Kit-8 migration assay

For the Cell Counting Kit-8 (CCK8) assay (Sigma, USA), HSFs (5×10^3 per well) were added to a 96-well plate, and cultured for 24, 48, or 72 h. Afterward, 20 μ L of CCK-8 reagent was added into cells in serum-free medium for 2 h, followed by measurements of absorbance at 450 nm.

Statistical analysis

GraphPad Prism 8.0 was used to calculate the data, which are presented as mean \pm standard deviation. Paired data were compared using *t* tests, and 1-way analysis of variance with Tukey's post hoc test was used to analyze data from 3 or more

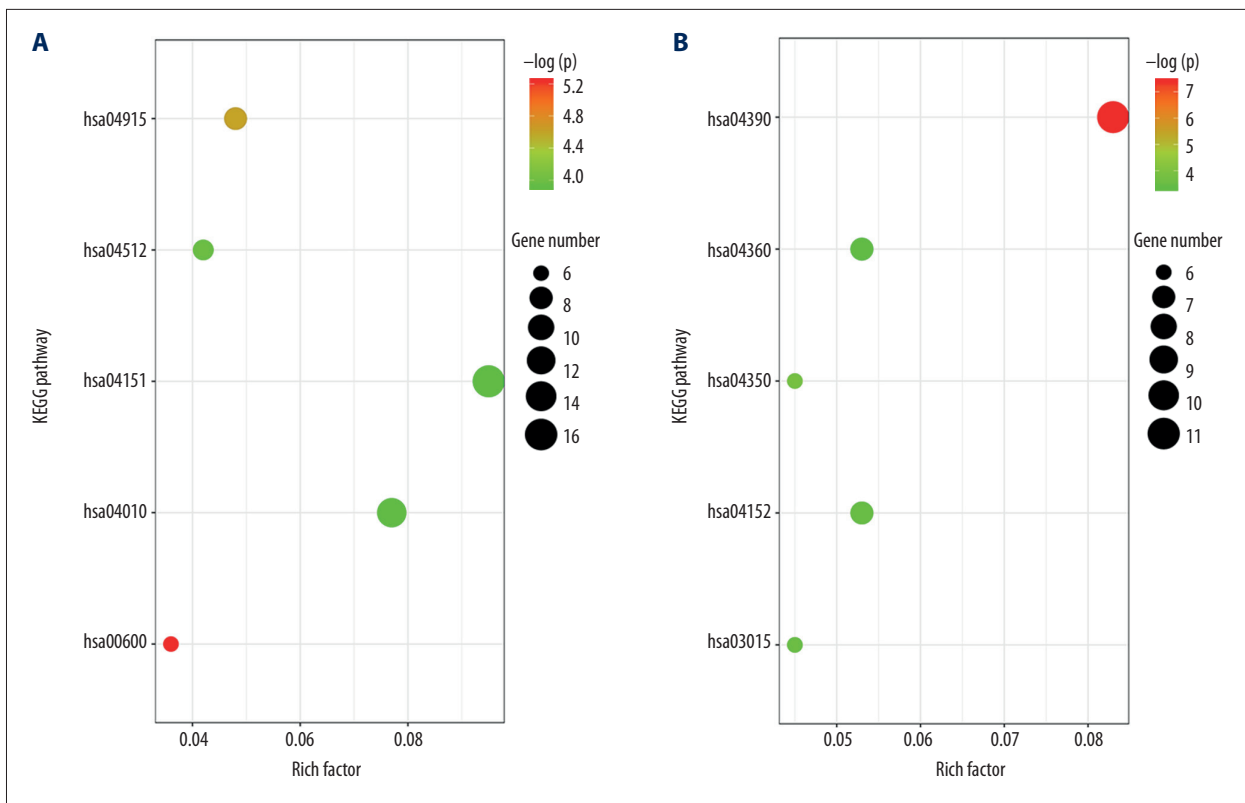


Figure 2. (A) Enrichment analysis results of upregulated genes: hsa00600, sphingolipid metabolism pathway; hsa04915, estrogen signaling pathway; hsa04512, ECM-receptor interaction pathway; hsa04010, MAPK signaling pathway; hsa04151, PI3K-Akt signaling pathway. (B) Enrichment analysis results of downregulated genes: hsa04390, Hippo signaling pathway; hsa04350, TGF- β signaling pathway; hsa03015, mRNA surveillance pathway; hsa04152, AMPK signaling pathway; hsa04360, Axon guidance pathway. ECM, extracellular matrix; MAPK, mitogen-activated protein kinase; PI3K-Akt, phosphatidylinositol-3-kinase and protein kinase B; TGF- β , transforming growth factor β .

groups. $P < 0.05$ was considered to indicate a statistically significant difference.

Results

Identification of DEGs

The gene expression profile GSE38396 was obtained from the GEO database. There were 8 samples in this microarray data, which included 4 normal individuals and 4 patients with type 2 diabetes. The 8 samples were analyzed with the Morpheus online tool, which identified 637 upregulated and 448 downregulated DEGs. The top 30 upregulated genes and top 30 downregulated genes are shown in Figure 1.

GO and KEGG analyses

GO analysis indicated that upregulated DEGs were significantly enriched in the following biological processes: positive regulation of GTPase activity, cardiovascular system development,

circulatory system development, positive regulation of hydrolase activity, and heart development. The downregulated DEGs were enriched in cell proliferation, reproductive structure development, reproductive system development, negative regulation of cell proliferation, and negative regulation of macromolecule metabolic processes (Table 1). With regard to cellular components, upregulated DEGs were significantly enriched in endosome lumen, axoneme part, endoplasmic reticulum lumen, vacuolar lumen, and late endosome lumen, whereas the downregulated DEGs were enriched in nucleoplasm, nucleoplasm part, adherens junction, anchoring junction, and stress fiber (Table 2). Among molecular functions, upregulated DEGs were significantly enriched in guanyl-nucleotide exchange factor activity, molecular function regulator, Ras guanyl-nucleotide exchange factor activity, inositol phosphate phosphatase activity, and pyridoxal-phosphate binding, whereas the downregulated DEGs were enriched in poly(A) RNA binding, nucleotide binding, nucleoside phosphate binding, small molecule binding, and carbohydrate derivative binding (Table 3).

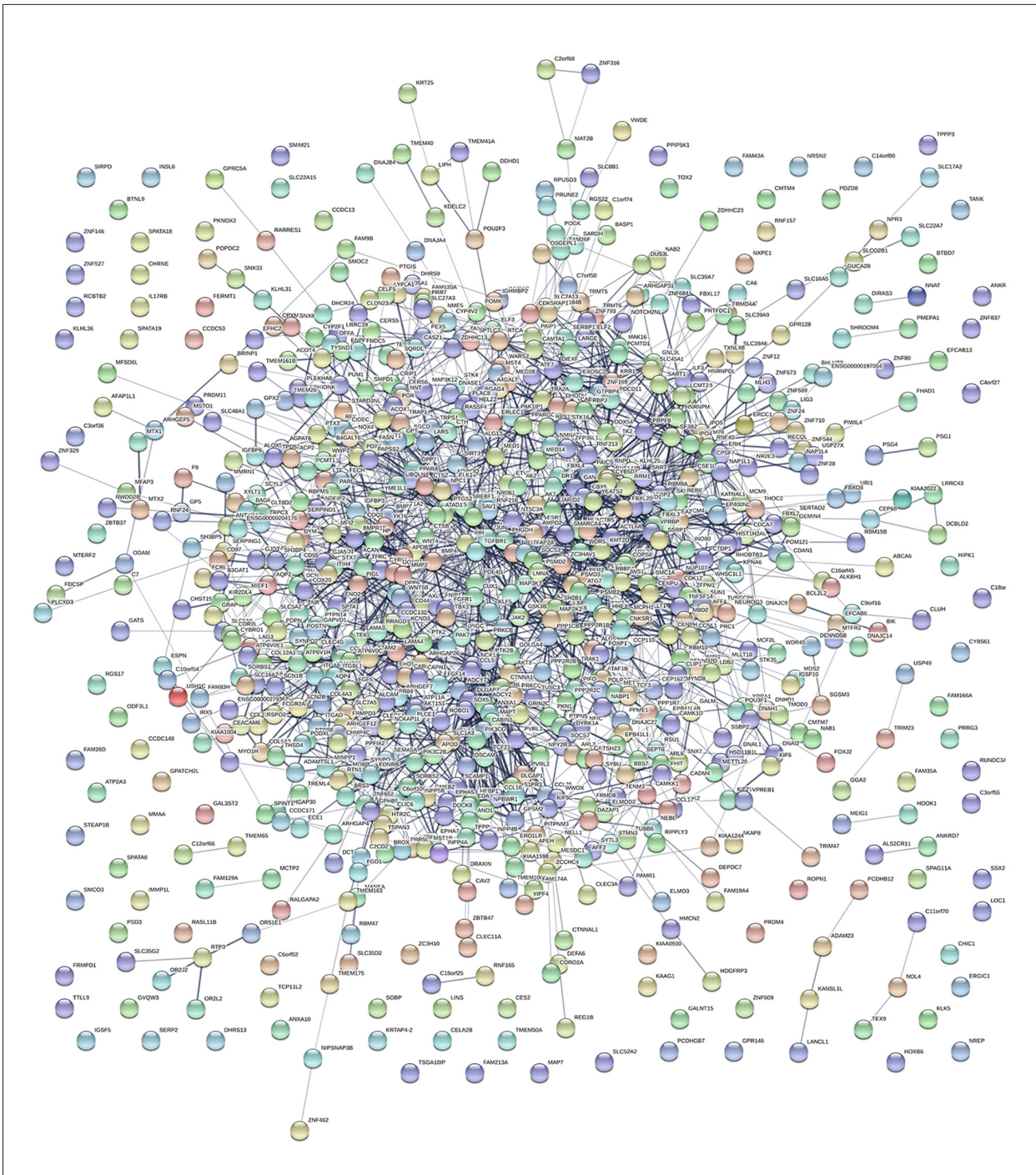


Figure 3. Interactions of the differentially expressed proteins. Protein–protein interaction (PPI) network constructed by STRING.

The top 5 KEGG pathways of upregulated DEGs were sphingolipid metabolism pathway, estrogen signaling pathway, ECM-receptor interaction pathway, MAPK signaling pathway, and PI3K-Akt signaling pathway. The top 5 KEGG pathways of downregulated DEGs were those for Hippo signaling, TGF-beta signaling, mRNA surveillance, AMPK signaling, and axon guidance (Table 4). The results of the KEGG enrichment analysis are shown in Figure 2.

PPI analysis

The PPI network was obtained using STRING (<https://string-db.org/cgi/input.pl>) (Figure 3), and the top 10 hub genes with high degrees were then obtained using Cytoscape. The hub genes included *JUN*, *ESR1*, *CD44*, *SMARCA4*, *MMP2*, *BMP4*, *GSK3B*, *WDR5*, *PTK2*, and *PTGS2* (Table 5). *JUN* had the highest degree,

Table 5. The top 10 genes by degree of association between one node and other nodes.

Gene ID	Gene name	Degree	Betweenness	Closeness
JUN	Jun proto-oncogene, AP-1 transcription factor subunit	48	51655	5.18E-4
ESR1	Estrogen receptor 1	36	31527	5.02E-4
CD44	CD44 molecule	36	27941	4.89E-4
SMARCA4	SWI/SNF related, matrix associated, actin dependent regulator of chromatin, subfamily A, member 4	34	29067	4.87E-4
MMP2	Matrix metalloproteinase 2	34	18562	4.85E-4
BMP4	Bone morphogenetic protein 4	32	14246	4.63E-4
GSK3B	Glycogen synthase kinase 3 beta	29	22274	4.86E-4
WDR5	WD repeat domain 5	29	21188	4.67E-4
PTK2	Protein tyrosine kinase 2	29	22879	4.63E-4
PTGS2	Prostaglandin-endoperoxide synthase 2	29	18796	4.76E-4

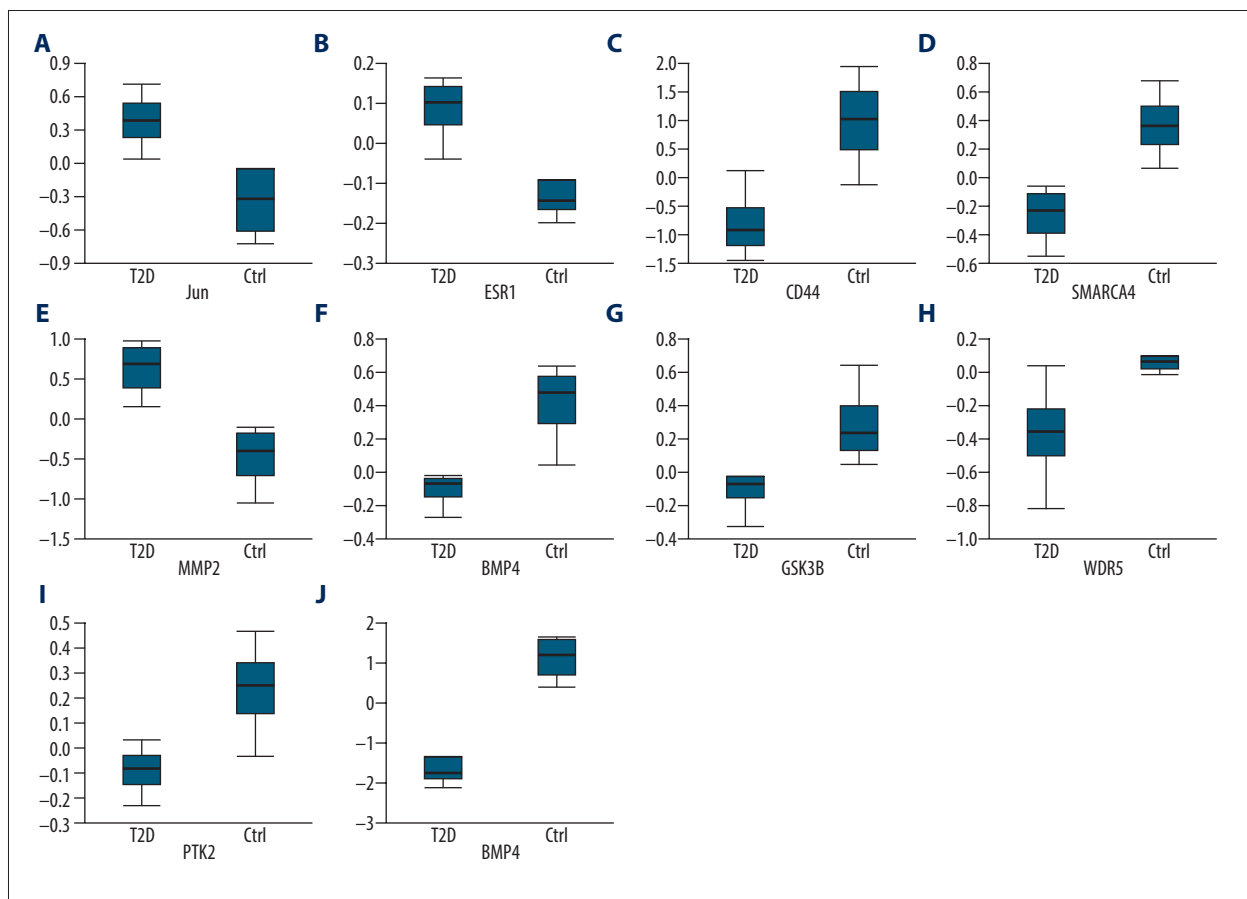


Figure 4. (A-J) Expression boxplot of *JUN*, *ESR1*, *CD44*, *SMARCA4*, *MMP2*, *BMP4*, *GSK3B*, *WDR5*, *PTK2*, and *PTGS2* visualized by Morpheus.

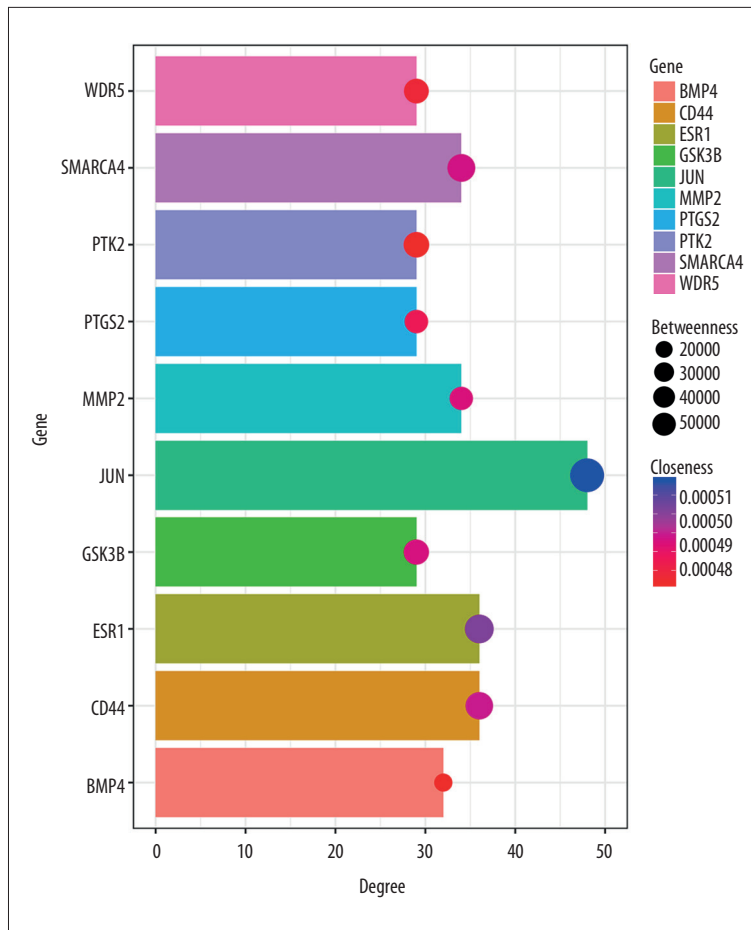


Figure 5. Degree, betweenness, and closeness of hub genes.

Table 6. Functional and pathway enrichment analyses of the genes in the protein–protein (PPI) network.

Term	Name	Count	P-value
A, Biological process			
GO: 0045597	Positive regulation of cell differentiation	66	1.7E-7
GO: 0072358	Cardiovascular system development	68	2.4E-6
GO: 0072359	Circulatory system development	68	2.4E-6
B, Cellular component			
GO: 0005654	Nucleoplasm	153	3.1E-3
GO: 0005578	Proteinaceous extracellular matrix	27	4.6E-3
GO: 0097517	Contractile actin filament bundle	8	6.7E-3
C, Molecular functions			
GO: 0098772	Molecular function regulator	84	6.7E-5
GO: 0008134	Transcription factor binding	39	1.2E-4
GO: 0005539	Glycosaminoglycan binding	20	5.2E-4
D, KEGG pathway			
hsa: 05205	Proteoglycans in cancer pathway	17	4.8E-3
hsa: 05200	Pathways in cancer	27	5.4E-3
hsa: 04390	Hippo signaling pathway	14	5.8E-3

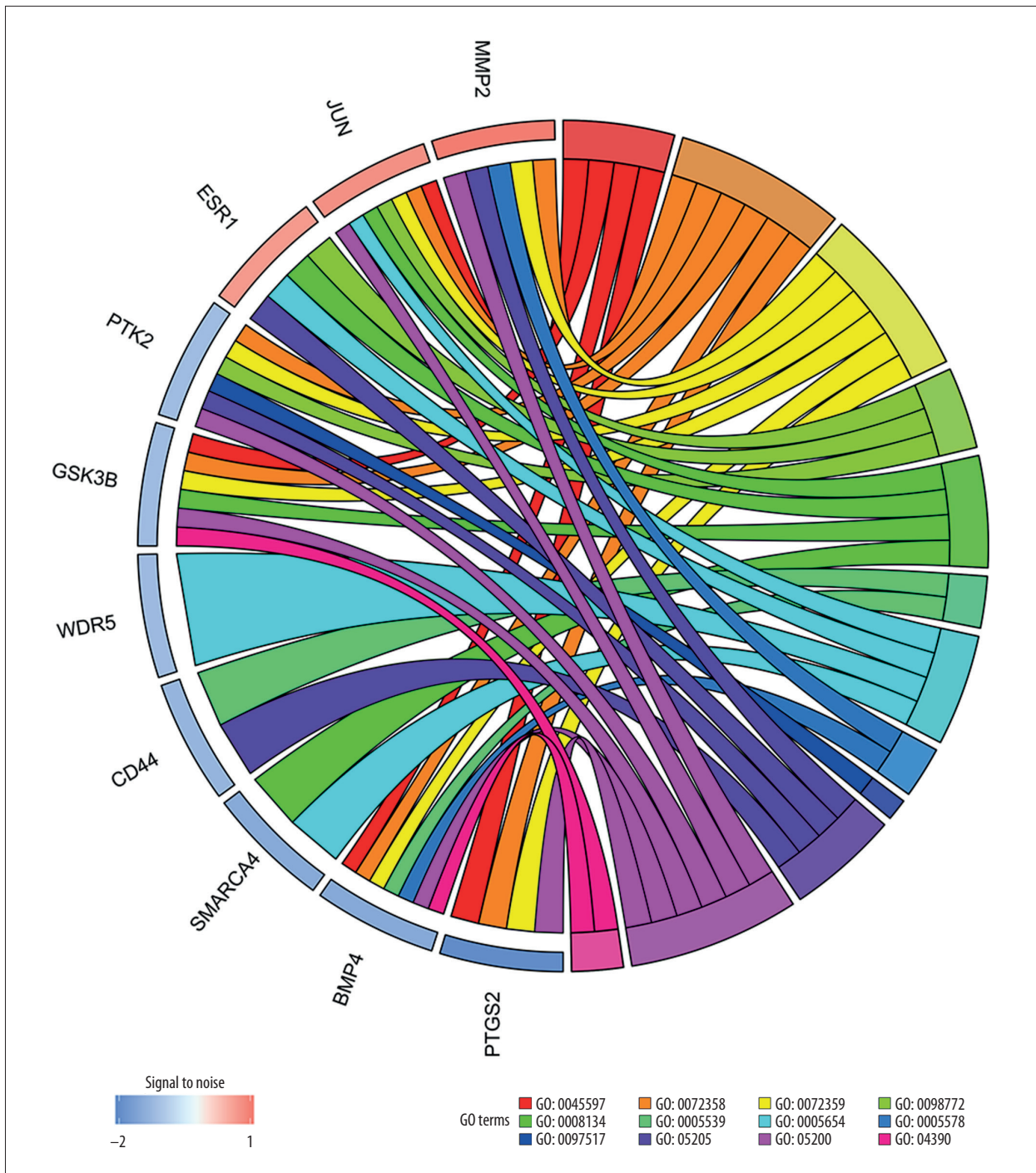


Figure 6. The enrichment of the top 10 genes in the protein–protein interaction (PPI) network. Biological processes: GO: 0045597, positive regulation of cell differentiation; GO: 0072358, cardiovascular system development; GO: 0072359, circulatory system development. Molecular functions: GO: 0098772, molecular function regulator; GO: 0008134, transcription factor binding; GO: 0005539, glycosaminoglycan binding. Cellular components: GO: 0005654, nucleoplasm; GO: 0005578, proteinaceous extracellular matrix; GO: 0097517, contractile actin filament bundle. KEGG pathway: hsa05205, proteoglycans in cancer pathway; hsa05200, pathways in cancer; hsa04390, Hippo signaling pathway.

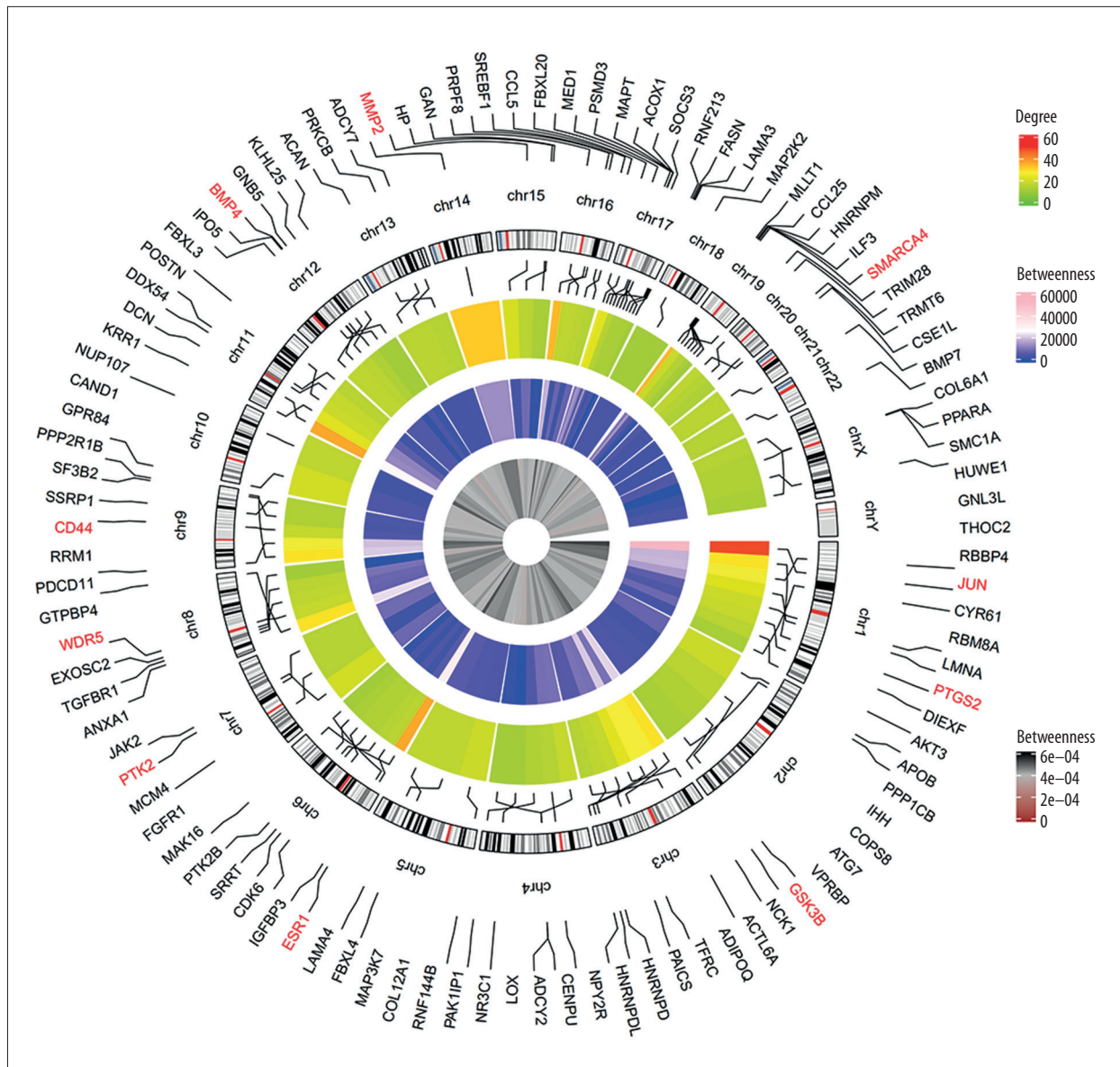


Figure 7. Circular visualization of chromosomal positions and connectivity of the top 100 genes in the protein-protein interaction (PPI) network. The names of the genes are shown in the outer circle. Different colors show different values of degree, betweenness, and closeness. The outer circle represents chromosomes; lines coming from each gene point to their specific chromosomal locations. The 10 hub genes are shown in red.

at 48. The expression boxplot of hub genes is shown in Figure 4. The degree, betweenness, and closeness of the hub genes are shown in Figure 5. The GO and KEGG pathway enrichment of the genes included in the PPI network showed that these genes were related to the biological processes of positive regulation of cell differentiation, cardiovascular system development, and circulatory system development; the molecular functions of molecular function regulator, transcription factor binding, and glycosaminoglycan binding; and the cellular components nucleoplasm, proteinaceous extracellular matrix, and contractile actin filament bundle. Most of the genes were enriched in

the following signaling pathways: proteoglycans in the cancer pathway, pathways in cancer, and the Hippo signaling pathway (Table 6). The enrichment of the top 10 genes is shown in Figure 6. The expression of the top 100 genes from the PPI network and their chromosomal positions are shown in Figure 7.

ESR1 was upregulated in patients with DWs and ESR1 inhibition enhanced HSF survival *in vitro*

The serum samples of the patients with DWs and the healthy controls were collected and quantitative real-time

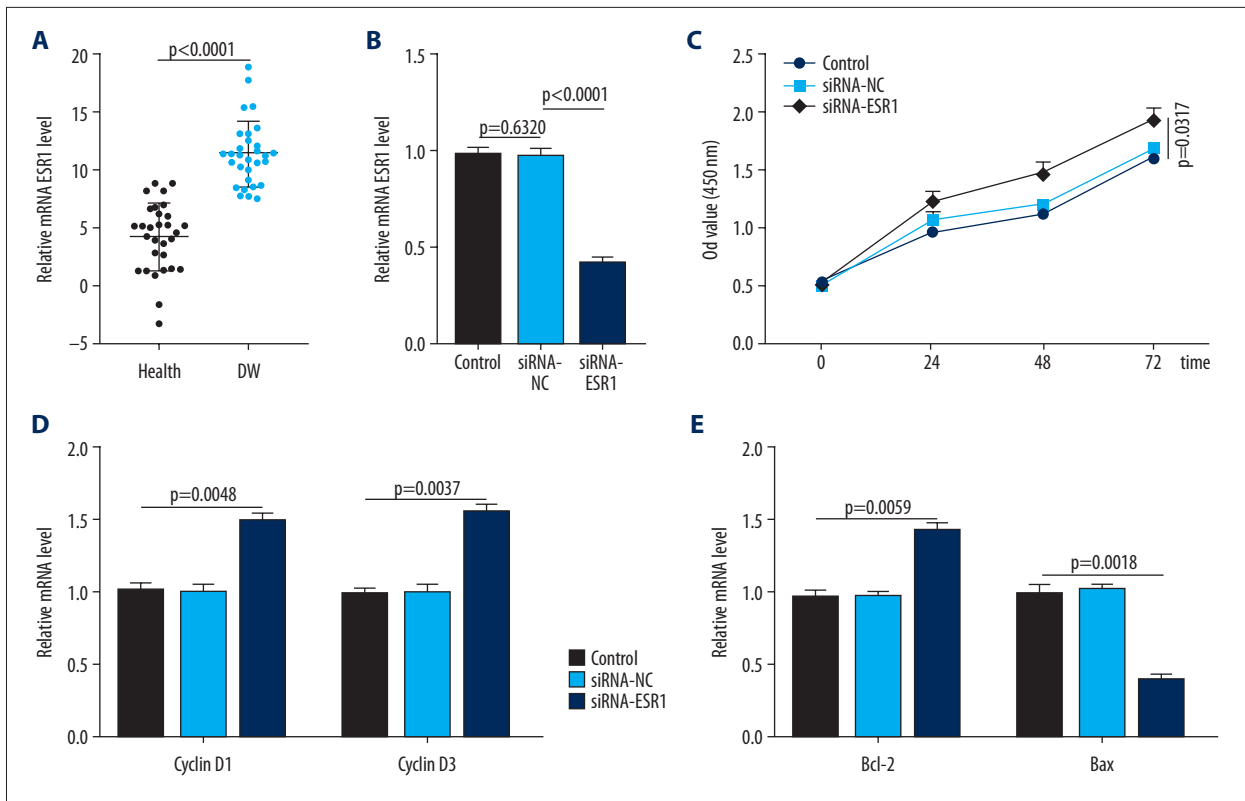


Figure 8. ESR1 is enriched in patients with diabetic wounds (DWs) and regulates human skin fibroblasts (HSFs). (A) The expression of ESR1 in the 2 groups was measured by quantitative reverse-transcription polymerase chain reaction (qRT-PCR) analysis, n=30 per group. (B) The expression of ESR1 in cell groups with different treatments was measured by qRT-PCR analysis. (C) The CCK-8 results of HSFs in different groups. (D) The levels of cyclin D1 and cyclin D3 in different groups were measured by qRT-PCR analysis. (E) The levels of Bcl-2 and Bax were measured by qRT-PCR analysis.

reverse-transcription polymerase chain reaction (qRT-PCR) analyses were performed to quantify *ESR1* expression in these samples. As shown in Figure 8A, *ESR1* was significantly upregulated in DW patients, which is consistent with the bioinformatic results. The effect of ESR1 on the proliferation of HSFs was then investigated *in vitro*. The CCK-8 assay showed that ESR1 inhibition promoted HSF proliferation (Figure 8B, 8C). Similarly, the qRT-PCR results indicated that the proliferation-related genes were increased and the apoptosis-related genes were decreased after *ESR1* knockdown treatment (Figure 8D, 8E).

Discussion

Many studies have focused on the mechanisms underlying DWs, and the identification of the key genes involved in DW development is a crucial step in these investigations [15]. In the present study, we screened for key genes associated with DW development, using mRNA expression datasets from DW and control patients. This analysis led to the identification of *JUN*, *ESR1*, *CD44*, *SMARCA4*, *MMP2*, *BMP4*, *GSK3B*, *WDR5*, *PTK2*, and *PTGS2* as potential key genes in diabetes; among these,

JUN, *MMP2*, and *ESR1* were upregulated. To explore whether these 3 genes were similarly enriched in patients with DWs, we carried out qRT-PCR analyses, which indicated that *JUN*, *MMP2*, and *ESR1* were significantly enriched in serum samples from the patients. Therefore, we hypothesized that *JUN*, *ESR1*, and *MMP2* are critical regulatory genes of DWs.

JUN is a protein coding gene, and diseases associated with *JUN* include pertussis and sarcoma [16]. Among its related pathways are the oxytocin signaling pathway and the CCR5 pathway in macrophages [17]. GO annotations related to this gene include sequence-specific DNA binding [18]. A recent study reported that the c-Jun/JNK/p53 signaling pathway is involved in the regulation of cardiac remodeling and apoptosis induced by myocardial infarction [19]. In the present study, we found that *JUN* is significantly upregulated in the diabetes based on the bioinformatic method, and it could be a key gene in DW development.

Matrix metalloprotein 2 (MMP2) has been reported to be involved in diverse functions, such as remodeling of the vasculature, angiogenesis, tissue repair, tumor invasion, inflammation, and atherosclerotic plaque rupture [20]. MMP2 was previously

demonstrated to be involved in the regulation of wound healing, and the upregulation of MMP2 was reported to accelerate cutaneous wound healing via enhancing the functionality of keratinocytes [21]. Interestingly, MMP2 was also demonstrated to be associated with the development of diabetes [22]. In the present study, MMP2 was found to be upregulated in diabetes, which is consistent with a prior study [23]. Thus, we regard MMP2 as another potential key gene in DW development.

Estrogen receptor 1 (ESR1) is a type of nuclear hormone receptor. The steroid hormones and their receptors are involved in the regulation of eukaryotic gene expression and affect cellular proliferation and differentiation in target tissues. Ligand-dependent nuclear transactivation involves either direct homodimer binding to a palindromic estrogen response element sequence or association with other DNA-binding transcription factors, such as AP-1/c-Jun, c-Fos, ATF-2, Sp1, and Sp3, to mediate estrogen response element-independent signaling [24]. A prior study reported that ESR1 was related to the molecular mechanisms of astragalus membranaceus for treating type 2 diabetes mellitus [25]. Fibroblasts are the key cells in cutaneous wound repair, and their proper function is essential for

wound contraction, collagen synthesis, and tissue remodeling. Therefore, we investigated how inhibition of ESR1 affects fibroblast function *in vitro*. We found that ESR1 is enriched in diabetes, and the qRT-PCR results indicated that ESR1 is also enriched in patients with DWs. In addition, inhibition of ESR1 was further demonstrated as useful for HSF survival. Considering our results, together with a recent study that demonstrated the effect of ESR1 in wound healing [26], we regard *ESR1* as a key gene in the regulation of DW healing.

Conclusions

In summary, the present study suggests that *ESR1* is a critical gene in the regulation of DW healing, which introduces potential therapeutic targets for DW healing. Although bioinformatics analysis and basic experimental tools were used to identify underlying crucial biomarkers of DW, the current study did not demonstrate the sensitivity and specificity of the key genes identified. However, from the bioinformatic and the cell-based analysis results, we assume that *ESR1* exerts a regulatory effect on DW healing via affecting the survival of fibroblasts.

References:

1. Argiana V, Kanellos PT, Eleftheriadou I et al: Low-glycemic-index/load deserts decrease glycemic and insulinemic response in patients with type 2 diabetes mellitus. *Nutrients*, 2020; 12(7): 2153
2. Xu Y, Cao K, Guo B et al: Lowered levels of nicotinic acetylcholine receptors and elevated apoptosis in the hippocampus of brains from patients with type 2 diabetes mellitus and db/db mice. *Aging (Albany NY)*, 2020; 12(14): 14205–18
3. Pratley R, Dagogo-Jack S, Charbonnel B et al: Efficacy and safety of ertugliflozin in older patients with type 2 diabetes mellitus: A pooled analysis of phase III studies. *Diabetes Obes Metab*, 2020 [Online ahead of print]
4. Xiong Y, Chen L, Yan C et al: Circulating exosomal miR-20b-5p inhibition restores Wnt9b signaling and reverses diabetes-associated impaired wound healing. *Small*, 2020; 16(3): e1904044
5. Xiong Y, Chen L, Yu T et al: Inhibition of circulating exosomal microRNA-15a-3p accelerates diabetic wound repair. *Aging (Albany NY)*, 2020; 12(10): 8968–86
6. Mi B, Chen L, Xiong Y et al: Saliva exosomes-derived UBE2O mRNA promotes angiogenesis in cutaneous wounds by targeting SMAD6. *J Nanobiotechnology*, 2020; 18(1): 68
7. Davis FM, denDekker A, Joshi AD et al: Palmitate-TLR4 signaling regulates the histone demethylase, JMJD3, in macrophages and impairs diabetic wound healing. *Eur J Immunol*, 2020 [Online ahead of print]
8. Xiong Y, Mi BB, Liu MF et al: Bioinformatics analysis and identification of genes and molecular pathways involved in synovial inflammation in rheumatoid arthritis. *Med Sci Monit*, 2019; 25: 2246–56
9. Yu T, You X, Zhou H et al: p53 plays a central role in the development of osteoporosis. *Aging (Albany NY)*, 2020; 12(11): 10473–87
10. Yu T, Wang Z, You X et al: Resveratrol promotes osteogenesis and alleviates osteoporosis by inhibiting p53. *Aging (Albany NY)*, 2020; 12(11): 10359–69
11. Xiong Y, Cao F, Chen L et al: Identification of key microRNAs and target genes for the diagnosis of bone nonunion. *Mol Med Rep*, 2020; 21(4): 1921–33
12. Huang DW, Sherman BT, Lempicki RA: Bioinformatics enrichment tools: Paths toward the comprehensive functional analysis of large gene lists. *Nucleic Acids Res*, 2009; 37(1): 1–13
13. Huang DW, Sherman BT, Lempicki RA: Systematic and integrative analysis of large gene lists using DAVID bioinformatics resources. *Nat Protoc*, 2009; 4(1): 44–57
14. Shannon P, Markiel A, Ozier O et al: Cytoscape: A software environment for integrated models of biomolecular interaction networks. *Genome Res*, 2003; 13(11): 2498–504
15. Tian C, Ouyang X, Lv Q et al: Cross-talks between microRNAs and mRNAs in pancreatic tissues of streptozotocin-induced type 1 diabetic mice. *Biomed Rep*, 2015; 3(3): 333–42
16. Yun SJ, Jun KJ, Komori K et al: The regulation of TIM-3 transcription in T cells involves c-Jun binding but not CpG methylation at the TIM-3 promoter. *Mol Immunol*, 2016; 75: 60–68
17. Hu J, Li S, Sun X et al: Stk40 deletion elevates c-JUN protein level and impairs mesoderm differentiation. *J Biol Chem*, 2019; 294(25): 9959–72
18. Srivastava M, Saqib U, Banerjee S et al: Inhibition of the TIRAP-c-Jun interaction as a therapeutic strategy for AP1-mediated inflammatory responses. *Int Immunopharmacol*, 2019; 71: 188–97
19. Lu L, Ma J, Sun M et al: Melatonin ameliorates MI-induced cardiac remodeling and apoptosis through a JNK/p53-dependent mechanism in diabetes mellitus. *Oxid Med Cell Longev*, 2020; 2020: 1535201
20. Diwanji N, Bergmann A: Basement membrane damage by ROS- and JNK-mediated Mmp2 activation drives macrophage recruitment to overgrown tissue. *Nat Commun*, 2020; 11(1): 3631
21. Zhang S, Zhu X, Li G: E2F1/SNHG7/miR-186-5p/MMP2 axis modulates the proliferation and migration of vascular endothelial cell in atherosclerosis. *Life Sci*, 2020; 257: 118013
22. Yang J, Zhao S, Tian F: SP1-mediated lncRNA PVT1 modulates the proliferation and apoptosis of lens epithelial cells in diabetic cataract via miR-214-3p/MMP2 axis. *J Cell Mol Med*, 2020; 24(1): 554–61
23. Nishihama K, Yasuma T, Yano Y et al: Anti-apoptotic activity of human matrix metalloproteinase-2 attenuates diabetes mellitus. *Metabolism*, 2018; 82: 88–99
24. Guclu-Geyik F, Coban N, Can G, Erginel-Unaltuna N: The rs2175898 polymorphism in the ESR1 gene has a significant sex-specific effect on obesity. *Biochem Genet*, 2020 [Online ahead of print]
25. Tan GC, Chu C, Lee YT et al: The influence of microsatellite polymorphisms in sex steroid receptor genes ESR1, ESR2 and AR on sex differences in brain structure. *Neuroimage*, 2020; 221: 117087
26. Moore K, Ghatnekar G, Gourdie RG, Potts JD: Impact of the controlled release of a connexin 43 peptide on corneal wound closure in an STZ model of type I diabetes. *PLoS One*, 2014; 9(1): e86570